JACS
JOURNAL OF THE AMERICAN CHEMICAL SOCIETY
Article
pubs.acs.org/JACS

Combined NMR Analysis of Huge Residual Dipolar Couplings and Pseudocontact Shifts in Terbium(III)-Phthalocyaninato Single Molecule Magnets

Marko Damjanovic,[†] Keiichi Katoh,[‡,§] Masahiro Yamashita,[‡,§] and Markus Enders*[,†]

[†]Institute of Inorganic Chemistry, University of Heidelberg, Im Neuenheimer Feld 270, D-69120 Heidelberg, Germany
[‡]Department of Chemistry, Graduate School of Science, Tohoku University, 6−3 Aramaki-Aza-Aoba, Sendai 980-8578, Japan
[§]JST, CREST, 4-1-8 Honcho, Kawaguchi, Saitama 332-0012, Japan

Supporting Information

ABSTRACT: Several small paramagnetic complexes combine large hyperfine NMR shifts with large magnetic anisotropies. The latter are a prerequisite for single molecule magnet (SMM) behavior. We choose the SMM tris(octabutoxy-phthalocyaninato) diterbium (**1**) for a high resolution NMR study where we combined for the first time a comprehensive ^{1}H and ^{13}C chemical shift analysis of a SMM with the evaluation of large residual dipolar couplings (RDCs). The latter are a consequence of partial alignment of SMM **1** in the strong magnetic field of the NMR spectrometer. To the best of our knowledge RDCs in SMMs have never been reported before. We measured RDCs between −78 and +99 Hz for the ^{13}C−^{1}H vectors of CH bonds and up to −109 Hz for ^{1}H−^{1}H vectors of geminal hydrogen atoms (magnetic field of 14.09 T, temperature 295 K). Considerable negative Fermi contact shifts (up to −60 ppm) were determined for ^{13}C atoms at the phthalocyaninato core. Paramagnetic ^{13}C NMR shifts of the butoxy chains as well as all ^{1}H NMR chemical shifts are a result of pseudocontact shifts (pcs), and therefore it is easily possible to determine the positions of the respective nuclei in solution. Measurements of CH and HH vectors by RDC analysis are in accordance with the geometry as determined by the pseudocontact shifts, but in addition to that, RDCs give information about internal mobility. The axial component of the magnetic susceptibility tensor has been determined independently by pcs and by RDC.

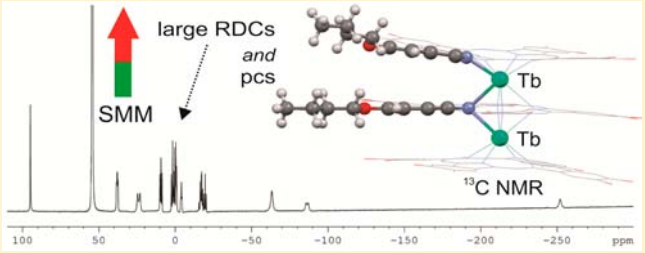

1. INTRODUCTION

Single molecule magnets (SMMs) are molecular materials displaying stable magnetization below a critical temperature. The prerequisite for SMM behavior is a high spin quantum number S combined with a large magnetic anisotropy ($\Delta\chi$), which leads to large zero-field splitting values D. In addition to that the sign of D must be negative. After the first description of SMM behavior in 1991,[1] numerous other systems have been published.[2] SMMs with only a single transition metal atom arise from highly anisotropic ions with strong spin−orbit coupling.[3] Recently the first SMM with a single d-block metal ion was reported, which consists of a high-spin Fe(II) complex of a bulky tetradentate ligand and a further improved linear Fe(I) complex.[4] SMM behavior is usually demonstrated by magnetic measurements at low temperatures. The sign and magnitude of the zero-field splitting parameter D can be determined by recording magnetization curves at different fields. Magnetic measurements, as well as almost all spectroscopic measurements with SMMs, are performed on solid samples.[5] Solution studies at room temperature are scarce. High-resolution ^{1}H NMR spectra of such highly paramagnetic samples have been reported in a few cases only and ^{13}C NMR spectra of such compounds have practically not been described.[6] The reason for that is the difficulty in recording and interpreting NMR spectra of highly paramagnetic compounds as a result of increased relaxation rates and extended chemical shift ranges. However, paramagnetic NMR spectroscopy could give valuable information for predicting SMM behavior because the paramagnetic susceptibility[7] and the anisotropy of the magnetic susceptibility tensor can be obtained quickly. The prerequisite for obtaining well-resolved paramagnetic NMR spectra is a fast relaxation of the electron Zeeman levels, which is the case for most lanthanide complexes but also for several d-block ions like high-spin Fe^{2+}.[8] The strong magnetic anisotropy of SMMs leads to paramagnetic NMR spectra with considerable pseudocontact shift (pcs) contributions.[9] Ishikawa fitted pcs data and SQUID magnetic measurement data of a series of lanthanide phthalocyaninato triple deckers in order to determine ligand field parameters.[6b−f] We have recently demonstrated that large residual dipolar couplings (RDCs) due to molecular alignment in the magnetic field can be analyzed in organometallic high-spin iron(II) complexes.[10] Therefore it is possible to obtain $\Delta\chi$ values independently by two effects in paramagnetic NMR

Received: July 8, 2013
Published: September 17, 2013

dx.doi.org/10.1021/ja4069485 | J. Am. Chem. Soc. 2013, 135, 14349−14358

spectroscopy, namely, the pseudocontact shift and RDC. Here we present the NMR analysis of the SMM terbium triple decker **1**, where strong pseudocontact shifts as well as huge residual dipolar couplings in ^{13}C NMR and in ^{1}H NMR can be observed. This compound combines high solubility, fast electron relaxation and high magnetic anisotropies. In addition to that, the molecule has axial symmetry so that pcs analysis as well as RDC analysis become easier since the rhombic terms are zero.

The analysis of pcs allows the determination of $\Delta\chi$ of the molecule. Because $\Delta\chi$ is also responsible for the molecular orientation in the magnetic field, it is linked to the observed RDCs. Additional mobility of substituents leads to decreases of $^{13}C-^{1}H$ or $^{1}H-^{1}H$ RDCs respectively, so that they are a measure of the mobility of the corresponding $^{13}C-^{1}H$ or $^{1}H-^{1}H$ vectors. In this work, we analyze comprehensively ^{1}H and ^{13}C NMR spectra of the triple decker SMM **1** shown in Figure 1.[11]

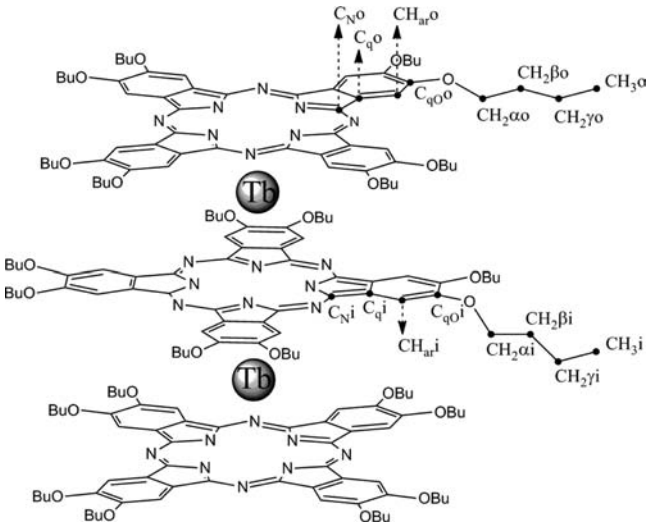

Figure 1. Schematic illustration of SMM **1** with the annotations used throughout this work.

2. THEORETICAL BACKGROUND

2.1. Contributions to the Chemical Shifts of Paramagnetic Compounds. Paramagnetic compounds lead to NMR spectra where the signals are strongly influenced by the interaction of the nuclear spins with the unpaired electron spins. The experimental chemical shift follows eq 1 (S is the spin multiplicity, β_e the Bohr magneton, γ_N the nuclear gyromagnetic ratio, and **g** and **A** are 3 × 3 matrices of the **g**- and **A**-hyperfine tensors, respectively):[12,13]

$$\delta_{\mathrm{obs},T} = \delta_{\mathrm{orb}} + \delta_{\mathrm{hf},T} = \delta_{\mathrm{orb}} + \frac{S(S+1)\beta_e}{3kT\gamma_N}\mathbf{gA} \quad (1)$$

The observed chemical shift ($\delta_{\mathrm{obs},T}$) can be expressed as the sum of the temperature-independent orbital term (δ_{orb}) and the temperature-dependent hyperfine term ($\delta_{\mathrm{hf},T}$). In diamagnetic compounds, the orbital shift (very commonly referred to as "diamagnetic shift") can be easily and accurately predicted. The hyperfine shift depends on the **g** and **A** tensors. The product of the matrices corresponding to the **g** and **A** tensors gives a variety of terms, some of which are purely isotropic, purely anisotropic, or both isotropic and anisotropic.[12e] In isotropic media, there are still a number of contributions to the hyperfine term, but it is dominated by only two terms, namely, the Fermi-contact shift (δ_{con} or δ_{fc}) and the pseudocontact shift (pcs or δ_{pc}). This has been verified by many NMR investigations in that field, even for $S > 1/2$ systems.[9,14] DFT calculations applying the recent general theory of the chemical shift in paramagnetic compounds support these experimental observations.[15] The pseudocontact shift arises from a dipolar interaction of the magnetic dipoles of the unpaired electrons and the nucleus. In a system where the magnetic susceptibility is axially anisotropic, pcs follows eq 2, where χ_a is the axial component of the magnetic susceptibility tensor (expressed in units of m^3), r is the length of the vector between the unpaired electrons (usually centered at the transition metal) and the NMR nucleus, and θ is the angle between the **r** vector and the magnetic field axis.

$$\delta_{\mathrm{pc}} = \frac{\chi_a}{12\pi r^3}(3\cos^2\theta - 1) \quad (2)$$

Hence it is possible to separate pcs from Fermi-contact interactions. The pcs can also be predicted by combining magnetic susceptibility measurements on single crystals with the geometric coordinates of the nuclei[12a] or by the direct use of the **g** tensor anisotropy.[16] Another possibility to separate pcs from Fermi-contact contributions is based on comparison of a series of lanthanide complexes of the same ligands.[17] The strong magnetic susceptibility anisotropy of complex **1** leads to large pseudocontact shift contributions. On the other hand, the Fermi-contact interaction is expected to be relatively weak in lanthanide complexes because unpaired f-electrons are delocalized to a smaller extent into the ligands, compared with unpaired d-electrons. This has been experimentally verified in many cases, and it turned out that Fermi-contact contributions are very small for ^{1}H whereas they may become larger for ^{13}C or $^{14/15}N$.[6,13,18] Due to the large χ_a of complex **1** and hence the large pcs, the observed chemical shifts can be approximated by eq 3:

$$\delta_{\mathrm{obs},T} \cong \delta_{\mathrm{orb}} + \delta_{\mathrm{pc},T} \quad (3)$$

Deviations from eq 3 due to Fermi-contact shift are only expected for the ^{13}C resonances of the phthalocyaninato moiety.

2.2. Residual Dipolar Couplings. The analysis of residual dipolar couplings (RDCs) is nowadays a well developed tool for structure determination of biomolecules in solution.[19] The intramolecular magnetic dipole−dipole interaction of nuclear spins, which is usually averaged out in solution, becomes visible in partially oriented media like nematic phases in liquid crystals or expanded gels. External electric or magnetic fields can also lead to a partial molecular alignment with emergence of RDCs, as has been first demonstrated by Lohman and MacLean.[20] However, the orientating forces of external magnetic fields are small so that ordering can be achieved only to a small extent. Consequently the RDCs are usually small. Paramagnetic molecules may have much larger magnetic anisotropies so that the ordering and hence the RDC can become larger. On the other hand, the line widths in NMR spectra of paramagnetic molecules can be very large, which may preclude the determination of RDC splittings. In larger paramagnetic molecules, such as metalloproteins, small RDCs can be measured more accurately as the line widths and relaxation behavior become favorable for positions distant from the paramagnetic center. Consequently, a detailed determination and analysis of $^{15}N-^{1}H$ RDCs was carried out with cyctochrome molecules aligned by their magnetic susceptibility anisotropy.[21]

The residual dipolar coupling between two $I = 1/2$ nuclei of a partially aligned molecule is expressed by eq 4.[22,23]

$$D_{\mathrm{AB}} = -\frac{\gamma_A\gamma_B\mu_0 h}{16\pi^3 r_{\mathrm{AB}}^3}\left[A_a(3\cos^2\theta - 1) + \frac{3}{2}A_r(\sin^2\theta\cos 2\varphi)\right] \quad (4)$$

where γ is the magnetogyric ratio of the respective nuclei, r_{AB} is the internuclear distance, A_a and A_r are the axial and rhombic components of the ordering tensor, and θ and φ describe the orientation of the internuclear bond vector relative to the alignment tensors.

Assuming a Boltzmann distribution of the orientations in an external magnetic field gives eqs 5a and 5b:

dx.doi.org/10.1021/ja4069485 | J. Am. Chem. Soc. 2013, 135, 14349−14358

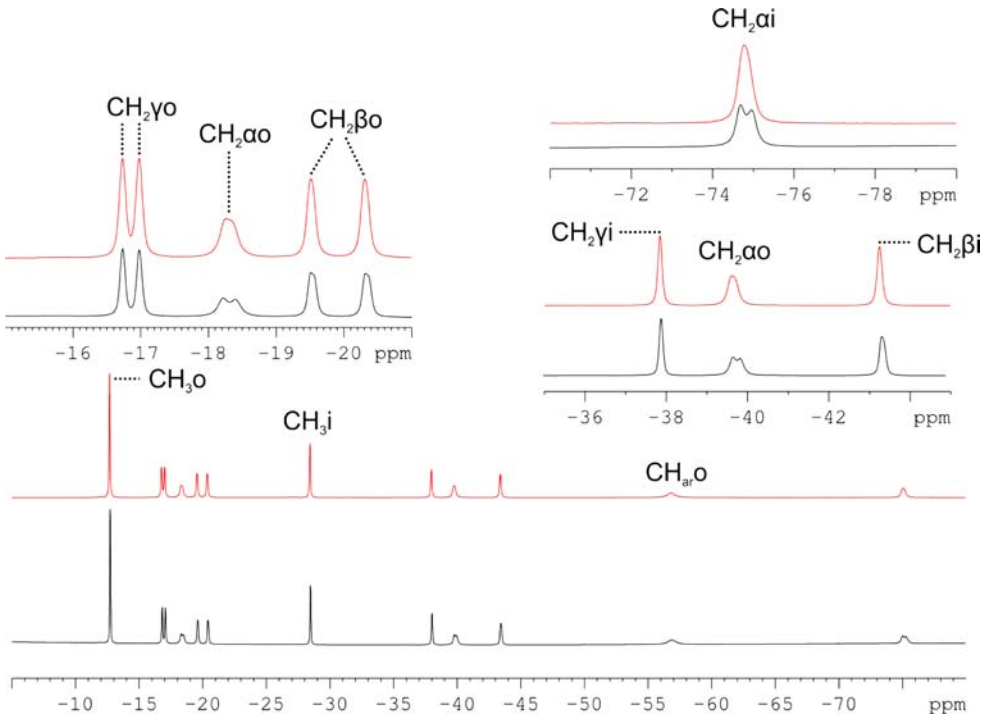

Figure 2. ^{1}H NMR spectrum of **1** recorded at 7.9 T (upper spectrum) and at 14.09 T (lower spectrum) in CD_2Cl_2 at 295.0 K, with selected enlarged segments and annotations of groups assigned to the resonances. For a full spectrum (containing the $CH_{ar}i$ resonance), please refer to Figure S1, Supporting Information.

$$A_a = \frac{\chi_a {B_0}^2}{15kT\mu_0} \quad \text{with} \quad \chi_a = \chi_{zz} - \frac{\chi_{xx} + \chi_{yy}}{2} \tag{5a}$$

$$A_r = \frac{\chi_r {B_0}^2}{15kT\mu_0} \quad \text{with} \quad \chi_r = \chi_{xx} - \chi_{yy} \tag{5b}$$

B_0 is the strength of the magnetic field, T is the applied temperature, k is the Boltzmann constant, μ_0 is the vacuum permeability, and χ_a and χ_r are the axial and rhombic components of the magnetic susceptibility tensor.

Upon combination of eqs 4 and 5 it is evident that the degree of molecular alignment and thus D_{AB} is proportional to the inverse temperature and the square of the applied magnetic field:

$$D_{AB} = -\frac{\gamma_A \gamma_B h}{16\pi^3 {r_{AB}}^3} \frac{{B_0}^2}{15kT}\left[\chi_a(3\cos^2\theta - 1) + \frac{3}{2}\chi_r(\sin^2\theta \cos 2\varphi)\right] \tag{6}$$

D_{AB} may be positive or negative depending on the orientation between the vector connecting the coupling nuclei and the principal magnetic axis. The temperature-dependent total multiplet splitting ($^1T_{CH}$) is the sum of the true scalar coupling ($^1J_{CH}$, approximately temperature-independent and always positive[24]) and the temperature-dependent RDC ($^1D_{CH}$). In some cases, the so-called dynamic frequency shift (DFS, see next section) leads to considerable contributions as well. Hence, eq 7 applies for $^1T_{CH}$:[25]

$$^1T_{CH}(T) = {}^1J_{CH} + {}^1D_{CH}(T) + {}^1\mathrm{DFS}_{CH}(T) \tag{7}$$

In ^{1}H NMR spectra, heteronuclear ^{13}C−^{1}H couplings are only present as low intensity satellites. Homonuclear ^nJ couplings are small and hence not observable in spectra with large line widths typical for small paramagnetic compounds. Consequently, large multiplet splittings originate from homonuclear RDCs, which give valuable information about ^{1}H−^{1}H vectors. Measurements at different magnetic fields (B_0) should give RDCs proportional to the square of B_0. For the methylene groups of the inner ring of complex **1**, the observed homonuclear $^1T_{HH}$ couplings are attributable to the RDCs only. For chemically equivalent protons, such as those of the aliphatic groups of the inner ring, the observed splitting amounts to 3/2 of the dipolar coupling.[20e] In the case of the methylene groups of the outer phthalocyaninato ring, geminal ^{1}H−^{1}H couplings should also be taken into consideration.[26]

2.3. The Dynamic Frequency Shift. The presence of hyperfine interaction between the electron and nuclear spins leads to a number of effects observable in NMR spectra of magnetically ordered materials.[27,28] The static part of the hyperfine interaction is manifested as a strong static magnetic field, whereas the fluctuating part of the hyperfine interaction leads to an enhancement of the external radio frequency field and to the Suhl−Nakamura interaction between the nuclear spins.[29,30] This interaction is one of the major sources of the broadening of NMR lines of magnetically ordered media and is also responsible for the dynamic frequency shift (DFS).[31,32] DFS is the clearest manifestation of the Suhl−Nakamura interaction, and it describes the deviation of the frequency of homogeneous precession of a nuclear spin N from the value $\gamma_N H_N$, where γ_N is the nuclear gyromagnetic ratio of nucleus N and H_N is the effective field strength.

As a way of describing the DFS in more detail, the differences in the relaxation rates of the components of, for example, a ^{13}C doublet (originating due to a coupling with ^{1}H) should be considered.[33] These differences in the relaxation rates arise due to the cross-coupling between the ^{1}H−^{13}C dipole−dipole and the chemical shift anisotropy relaxation mechanisms. The ^{13}C chemical shift anisotropy can be assumed to be axial along the ^{13}C−^{1}H internuclear vector. In such instances, the two ^{13}C doublet components have different spectral densities. The imaginary parts of the spectral densities are responsible for slight changes in the resonance frequencies of the doublet components. Because the imaginary parts of the spectral densities are different for the two components of the ^{13}C doublet, the resonance frequencies differ from each other and lead to an additional contribution to the $^1T_{CH}$ coupling. For a precise measurement of residual dipolar couplings of paramagnetic systems, dynamic frequency shifts should be taken into consideration.[34] The mathematical equations necessary for the calculation of DFS have been adapted

dx.doi.org/10.1021/ja4069485 | J. Am. Chem. Soc. 2013, 135, 14349−14358

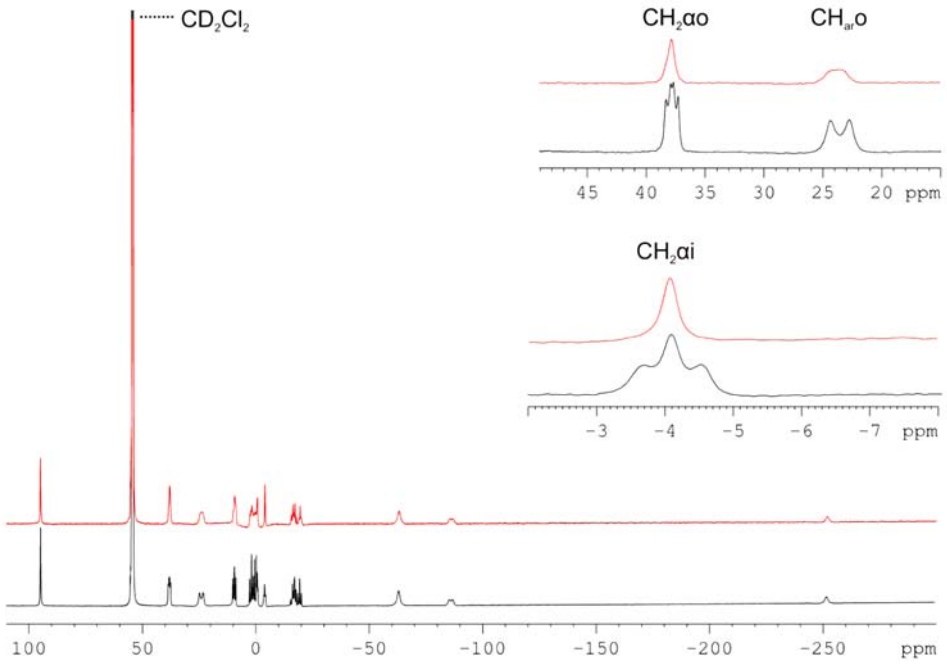

Figure 3. ^{13}C NMR spectrum (lower) and ^{13}C $\{^1H\}$ NMR spectrum (upper) of **1** recorded at 14.09 T, in CD_2Cl_2, at 295.0 K, with selected enlarged regions and assignments. For a more detailed ^{13}C NMR spectrum with full assignments, see Figure S3, Supporting Information.

from those reported by Ghose and Prestegard[35] and are given in the Supporting Information.

3. RESULTS

3.1. Assignment of ^{13}C and ^1H NMR Spectra. Figure 2 shows the ^1H NMR spectra of **1** recorded at 7.9 T and at 14.09 T. ^1H NMR spectra at 7.05 T have been reported for heteroleptic triple decker complexes of terbium with phthalocyanines but without the observation of D_{HH} couplings.[6e]

All expected ^1H NMR resonances are visible, and the chemical shift can be analyzed by the dominating pcs. The atoms of the inner phthalocyaninato ligand are influenced by two equivalent terbium centers so that the pcs values for these positions are about twice as large compared with the atoms of the outer ligands. The two ^1H NMR signals of the methylene groups of the inner ring are equivalent due to the symmetry plane along the inner phthalocyaninato ligand whereas the corresponding outer methylene groups are diastereotopic and give rise to two signals. These assignments are supported by corresponding carbon peaks in the ^1H, ^{13}C correlation spectrum (Figure S2, Supporting Information). The observed splittings in the ^1H NMR spectrum recorded at 14.09 T (barely noticeable in the 7.9 T ^1H NMR spectrum) are due to residual dipolar couplings, which will be analyzed later.

The ^{13}C resonances of the inner phthalocyaninato ligands, when compared with the ^{13}C resonances of the outer ligands, also show pcs values that differ by a factor close to 2. The ^{13}C and ^{13}C $\{^1H\}$ NMR spectra of **1** dissolved in CD_2Cl_2, recorded at 14.09 T at 295.0 K, are shown in Figure 3.

Assignments of all ^1H and ^{13}C resonances were confirmed with a ^1H, ^{13}C correlation experiment, as mentioned above, and are reported in Table 1.

3.2. Analysis of Pseudocontact Shifts. Considering that the triple decker **1** contains two terbium ions, eq 2 takes the following form:

Table 1. Observed (δ_{obs}) ^1H and ^{13}C NMR Chemical Shifts of 1 Recorded in CD_2Cl_2, at 295.0 K and the Corresponding Hyperfine Shifts (δ_{hf}), Calculated as $\delta_{hf} = \delta_{obs} - \delta_{orb}$[a]

group	δ_{obs} in ^1H NMR [ppm]	δ_{hf} in ^1H NMR [ppm]	δ_{obs} in ^{13}C NMR [ppm]	δ_{hf} in ^{13}C NMR [ppm]
$CH_2\alpha i$	−75.17	−79.23	−4.1	−72.8
$CH_2\beta i$	−43.43	−45.19	−17.4	−49.2
$CH_2\gamma i$	−38.02	−39.47	−19.6	−38.6
$CH_3 i$	−28.47	−29.37	−16.7	−30.8
$C_q i$			−252.1	−365.9
$CH_{ar} i$	−167.19	174.69	−86.5	−200.0
$C_{qO} i$			−0.8	−151.1
$CH_2\alpha o$	−18.39; −39.87	−22.45; −43.93	37.9	−30.8
$CH_2\beta o$	−19.60; −20.40	−21.36; −22.16	9.3	−22.5
$CH_2\gamma o$	−16.82; −17.07	−18.27; −18.52	1.7	−17.3
$CH_3 o$	−12.72	−13.62	0.0	−14.1
$C_q o$			−63.3	−177.1
$CH_{ar} o$	−56.90	−64.40	23.8	−89.7
$C_{qO} o$			94.8	−55.5

[a]Values of the orbital shifts were taken from calculations.

$$\delta_{pc} = \frac{\chi_a}{12\pi}\left(\frac{(3\cos^2\theta_{prox} - 1)}{r_{prox}^3} + \frac{(3\cos^2\theta_{dist} - 1)}{r_{dist}^3}\right) \quad (8)$$

where r_{prox} and r_{dist} are the lengths of the vectors connecting the proximal and distal terbium ions to the NMR nucleus and θ_{prox} and θ_{dist} are the corresponding angles between the r vectors and the magnetic field (Tb−Tb) axis. For the atoms of the inner phthalocyaninato ligand, in an idealized case, the values of the θ angles and r vector lengths relative to the two terbium ions are equivalent; hence eq 8 becomes

$$\delta_{pc} = \frac{\chi_a}{6\pi}\frac{(3\cos^2\theta - 1)}{r^3} \quad (9)$$

dx.doi.org/10.1021/ja4069485 | J. Am. Chem. Soc. 2013, 135, 14349−14358

The $(3\cos^2\theta - 1)/r^3$ terms are from here on referred to as the geometric factors. The values of the diamagnetic chemical shifts needed to calculate the pcs contribution to the total chemical shift were calculated incrementally for the phthalocyaninato ligand of **1** (Table S3, Supporting Information). When a series of isostructural complexes is available, the orbital contributions to the total chemical shifts and the values of the scalar couplings can be obtained from the NMR spectra of the diamagnetic members of the series. For complex **1**, diamagnetic analogues are octabutoxyphthalocyaninato complexes with La(III) or Lu(III) metal centers.[36]

After the successful assignment of all the observed ^{13}C and ^{1}H resonances, we proceeded with the calculation of the magnetic susceptibility anisotropy of **1** dissolved in d^2-dichloromethane, using the experimentally obtained values of the ^{13}C pseudocontact shifts. For such an approach, it was important to select the carbon atoms that have a negligible Fermi-contact contribution. This excluded the C_q, CH_{ar}, and C_{qO} groups from being considered for the calculation of χ_a. The C atom positions of the inner butoxy chain are better defined as compared with the outer chain, and therefore we choose the inner butoxy chain of **1** for the determination of the magnetic susceptibility anisotropy.

The χ_a value of **1** dissolved in deuterated dichloromethane was determined in the following manner.

The overall geometric factor (sum of the two geometric factors for each of the terbium centers of eq 8) for the three groups $CH_2\alpha$i, $CH_2\beta$i, and $CH_2\gamma$i was calculated using the available X-ray structure.[11] The experimental pseudocontact shifts were then used for the calculation of χ_a. For a full account of all the coordinates used in the calculation of the χ_a and its standard deviation, refer to Tables S4−S6, Supporting Information. The average of the χ_a values calculated in this way is $(10.15 \pm 0.37) \times 10^{-31}$ m^3 at 295.0 K. χ_a values calculated at all temperatures are provided in Table S7, Supporting Information.

With the magnetic susceptibility anisotropy now available, we proceeded with the further interpretation of our data using the calculated χ_a values. The initial model was refined in order to account for signal averaging due to the presence of different conformers and molecular motion. The refined model has slightly deviating C−C bond lengths and C−C−C and C−C−O angles of the inner and outer butoxy groups (Table S8, Supporting Information). For the outer butyl chain, the dihedral angles were fitted with the experimental ^{13}C pseudocontact shifts, taken from the ^{13}C NMR spectrum recorded at 295.0 K.[37] As expected, the fit shows that this alkyl chain tends to point away from the rest of the molecule, in such a way that the chain and the z axis of the molecule (magnetic field axis) enclose an angle of approximately 75°. The fitted dihedral angles are given in Table S9, Supporting Information.

Because of the axial symmetry of **1**, several constraints were introduced for the inner BuO chain. Using the diameter of the inner phthalocyaninato ligand of the complex, we first symmetrized the X-ray data for the positions of the C_qi, CH_{ar}i, and C_{qO}i carbons and the oxygen atom attached to C_{qO}i, in such a way that these carbons were equidistant from both terbium ions. We attached the butyl chain, while setting all the dihedral angles to either zero or 180°, that is, making $CH_2\alpha$i, $CH_2\beta$i, $CH_2\gamma$i, and CH_3i equidistant from either terbium center. The carbon−hydrogen distances in all methylene and methyl groups were fixed to 1.093 Å and the H−C−H angles were fixed to 109.5°. The carbon−hydrogen bond lengths of the CH_{ar}o and CH_{ar}i groups were fixed to 1.081 Å. These values correspond to neutron diffraction data of comparable structural elements.[38]

The calculated ^{13}C pseudocontact shifts using the above-mentioned model were plotted against the experimentally determined paramagnetic shifts at 295.0 K (see Figure 4).

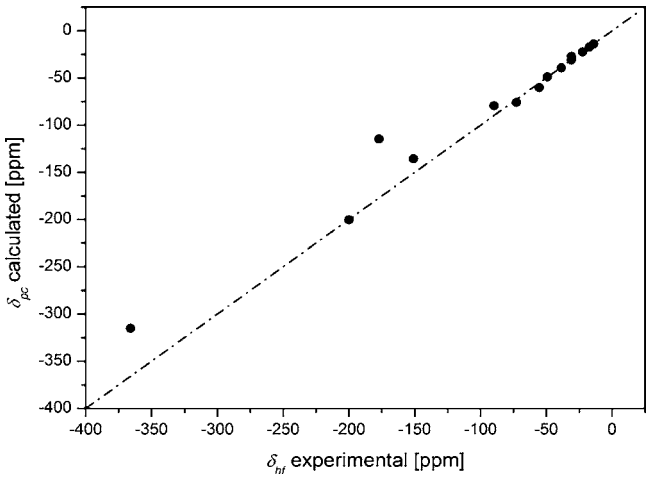

Figure 4. Calculated pseudocontact shifts vs experimental paramagnetic shifts of the ^{13}C resonances of **1** dissolved in deuterated dichloromethane at 295.0 K. The dash-dot line represents the δ_{pc} (calculated) = δ_{hf} (experimental) line. Corresponding plots for different temperatures, a full list of coordinates, and pseudocontact shifts are given in Figures S14−S18 and Tables S10 and S11 and S12, respectively.

The presented model, created to fit the ^{13}C NMR pcs data at 295.0 K, is also valid for all other temperatures at which ^{13}C NMR spectra were recorded. The model represents an average of relevant conformations of the BuO chain in solution. The outliers from the diagonal belong to the aromatic carbon atoms. These are the resonances for which we expect a considerable Fermi-contact contribution to the overall hyperfine shift. The differences between the outliers and the diagonal in Figure 4 are separately presented in Figure 5 and can be attributed to the Fermi-contact term.

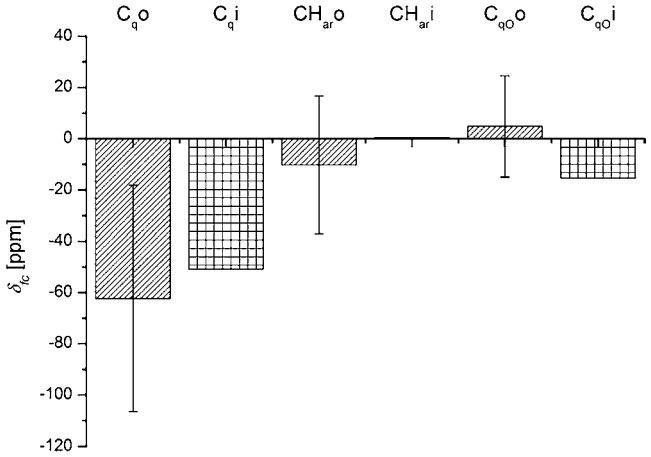

Figure 5. Fermi-contact contributions to the hyperfine shift of the aromatic carbon atoms of **1** dissolved in deuterated dichloromethane at 295.0 K.

dx.doi.org/10.1021/ja4069485 | J. Am. Chem. Soc. 2013, 135, 14349−14358

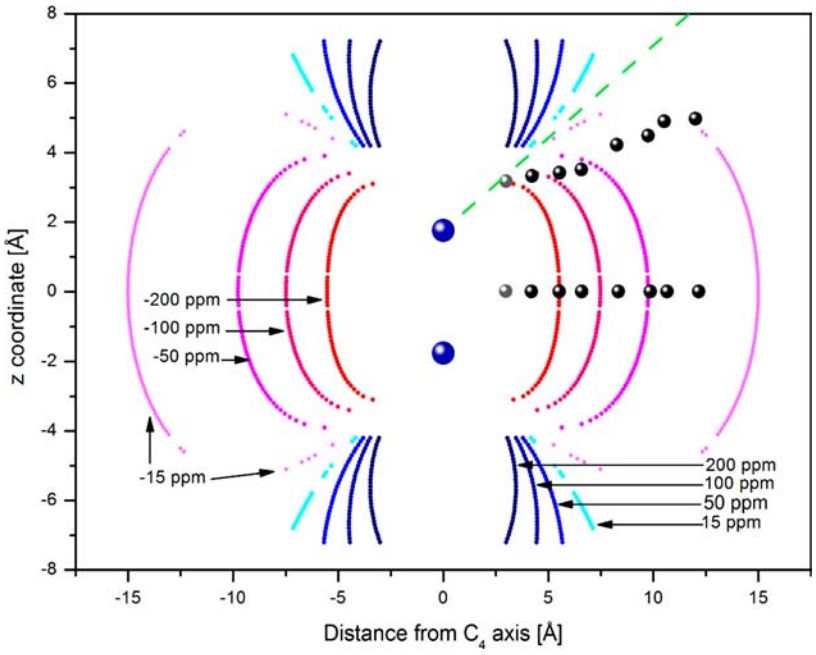

Figure 6. Isointensity plots for pcs calculated for complex **1** dissolved in CD_2Cl_2 at 295.0 K, with inserted carbon atoms from the refined model (represented by black spheres). The calculation was conducted as explained in the Supporting Information. Regions where the pseudocontact shifts are negative are marked with a red to pink color gradient, whereas regions where these shifts have a positive value are marked with a deep blue to lime color gradient. Carbon atoms marked in light gray (C_Ni and C_No from Figure 1) were not observed in ^{13}C NMR spectra. The positions of the terbium ions are indicated by the larger, deep blue spheres. The green dashed line represents the region where the pseudocontact shift changes sign.

Figure 5 is fairly consistent with the expected behavior of the Fermi-contact shift for the ^{13}C nuclei of the inner phthalocyaninato ligand: The largest δ_{fc} is observed for the carbon nuclei closest to the terbium centers; C_qi and C_{qO}i show negative Fermi-contact shifts, because these are separated from each terbium center by an odd number of bonds; the CH_{ar}i group has an even number of bonds separating it from each of the terbium ions and shows a slightly positive Fermi-contact shift. Because the outer aromatic carbon atoms display pseudocontact as well as Fermi-contact shifts, we could not fit the exact positions of these atoms for the outer ring. The X-ray data showed considerable differences of the eight individual carbon atoms, and these differences are presented as error bars in Figure 5. Hence, for the outer ring, we can only state that the C_qo carbons have a negative Fermi-contact shift of the same order of magnitude as that of the C_qi carbons and that the CH_{ar}o and C_{qO}o carbons have small Fermi-contact shift contributions to the overall chemical shift. The coordinates of the C_qi, CH_{ar}o, and C_{qO}o carbons, as taken from the crystal structure of complex **1**, are given in Table S13, Supporting Information; the calculated ^{13}C pseudocontact shifts based on these coordinates are given in Table S14, Supporting Information, and the ^{13}C Fermi-contact contributions obtained at all temperatures are given in Table S15, Supporting Information.

We applied the same model as established for a solution of **1** in deuterated dichloromethane to a ^{13}C NMR spectrum of complex **1** in toluene-d^8, recorded at 14.09 T, at a temperature of 295.0 K. The model is in very good agreement with the experimental data. The Fermi-contact contributions for this sample followed a similar trend as that presented in Figure 5. In the case of toluene-d^8 as the solvent, the χ_a of **1** calculated as stated above equals $(8.52 \pm 0.22) \times 10^{-31}$ m^3. Spectra and chemical shift data related to the sample dissolved in toluene-d^8 are provided in Figures S19–S21 and Tables S16 and S17, Supporting Information.

Upon inspection of the pseudocontact shift data, it becomes apparent that all observed carbon atoms in **1** have a negative pseudocontact shift contribution (Table 1). This confirms that the triple decker molecule is aligned in solution in such a way that the Tb–Tb vector is parallel to the magnetic field axis. To further exemplify this, we have calculated isointensity plots for our complex dissolved in deuterated dichloromethane, using the magnetic susceptibility anisotropy value calculated at 295.0 K. The isointensity plot is presented in Figure 6.

In Figure 6, it is apparent that the C_No carbon atom lies in the region where slight displacements of the position lead to very large changes in the pseudocontact shift contributions to the overall chemical shift. The C_Ni and C_No carbon atoms are unobserved in the NMR spectra. A likely cause for this is the fast relaxation of these nuclei, since they are in proximity to the metal centers. Coordinates of the C_No and C_Ni carbon atoms, along with their predicted pseudocontact shift values, are presented in Tables S18 and S19, respectively. Figure 6 also justifies our approach to calculate the magnetic susceptibility anisotropy of **1** using the carbon atoms of the inner phthalocyaninato ligand only. Namely, as the isointensity lines of this figure show, displacements of the carbon atoms of the inner ligand along the z coordinate would lead to very small changes in the pseudocontact shift values, that is, a carbon atom would still be on the same isointensity line. On the other hand, the carbon atoms of the outer ligand lie in a region where even very small displacements along the z axis could lead to noticeable changes in the values of the pseudocontact shifts.

We proceeded to calculate δ_{pc} values of the ^{1}H nuclei, whose positions were fixed because of the predetermined carbon scaffold that was fitted to our ^{13}C NMR data. The calculated ^{1}H pseudocontact shifts are shown compared with the exper-

dx.doi.org/10.1021/ja4069485 | J. Am. Chem. Soc. 2013, 135, 14349–14358

imentally determined values at 295.0 K in Figure 7. The coordinates of the protons for the applied model are given in Table S20, Supporting Information.

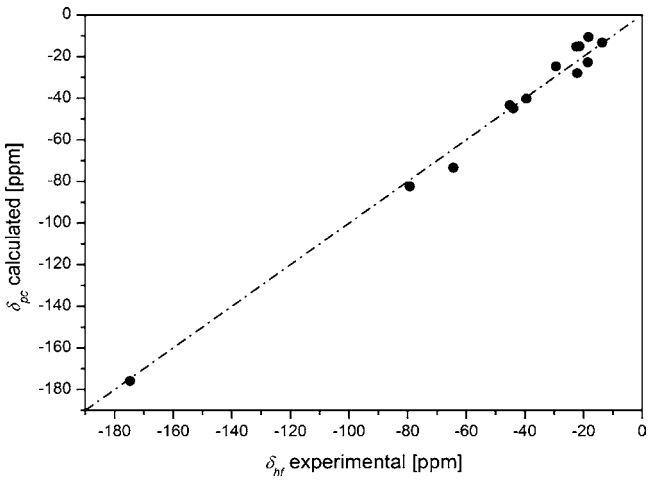

Figure 7. Calculated pseudocontact shifts vs experimental paramagnetic shifts of the ^{1}H resonances of **1** dissolved in deuterated dichloromethane at 295.0 K. The dash-dot line represents the δ_{pc} (calculated) = δ_{hf} (experimental) line.

Figure 7 shows a good correlation between the experimentally observed δ_{pc} values and values calculated from the model used to fit the ^{13}C NMR data. The same model holds for all the temperatures at which measurements were conducted (Tables S21 and S22, Supporting Information). The differences between the calculated δ_{pc} and experimental δ_{hf} values for the protons in the inner and outer BuO chains are on the order of max 8 ppm. These differences, when translated into the positions of the ^{1}H nuclei, actually represent minor changes from the utilized model.

3.3. Analysis of ^{13}C−^{1}H and ^{1}H−^{1}H Couplings.

3.3.1. Dynamic Frequency Shifts. Values of $^1T_{CH}$ and $^1T_{HH}$ were extracted from the ^{13}C NMR and ^{1}H NMR spectra, respectively, and are given in Tables S23 and S24, Supporting Information. Due to the broadness or overlap of some of the signals, the errors in extracting the total couplings have been estimated and are given in Table S25, Supporting Information, for the $^1T_{CH}$ and Table S26, Supporting Information, for the $^1T_{HH}$. We applied eq S7, Supporting Information, to calculate the DFS contributions to the total couplings in ^{13}C NMR spectra. The coordinates needed for this equation were taken from the above-mentioned model and are made available in Table S27, Supporting Information, and the Larmor frequencies used in the calculations are reported in Table S28, Supporting Information. DFS contributions calculated at all temperatures are provided in Table S29, Supporting Information. The correlation time for overall molecular tumbling was estimated using Stokes' law (e.g., 1.09 ns at 295 K in CD_2Cl_2 solution, see Supporting Information). For the ^{13}C−^{1}H couplings observed in ^{13}C NMR spectra, dynamic frequency shifts were on the order of −11 to −32 Hz for the aromatic CH groups and on the order of −1 to −8 Hz for the groups of BuO chains, decreasing in magnitude toward the methyl groups. All of the calculated DFSs have a negative sign. The relevance of the calculated DFSs is evident from the values given in Table 2.

Table 2. Experimental Total Splittings ($^1T_{CH}$ and $^1T_{HH}$, respectively), Calculated DFS ($\Delta\nu_{DFS}$) and Extracted RDCs (D_{CH} and D_{HH})

		^{13}C NMR data			^{1}H NMR data	
group	comments	$^1T_{CH}$ [Hz]	$\Delta\nu_{DFS}$ [Hz]	D_{CH} [Hz]	$^1T_{HH}$ [Hz]	D_{HH} [Hz]
$CH_2\alpha$i		65.0	−4.0	−72.0	−163.3	−108.9[c]
$CH_2\beta$i		94.0	−3.2	−27.8	−21.6	−14.4[c]
CH_2yi		113.4	−3.1	−8.5		
CH_3i		116.5	−1.5	−7.0		
CH_{ar}i		223.0	−20.5	85.1		
$CH_2\alpha$o	farther ^{1}H[a]	58.0	−5.2	−77.8	−105.6	−94.4[d]
	closer ^{1}H[a]	96.0	−2.6	−42.4	−104.7	
$CH_2\beta$o	farther ^{1}H[a]	113.0	−1.8	−10.2	−31.8	−19.4[d]
	closer ^{1}H[a]	95.0	−3.4	−26.6	−31.7	
CH_2yo	*b*	121.6	−2.7	−1.2		
	b		−1.7	−1.2		
CH_3o		118.4	−1.1	−5.5		
CH_{ar}o		242.0	−15.1	98.7		

[a]The two ^{13}C−^{1}H vectors of the methylene groups of the outer phthalocyaninato ligand show different residual dipolar couplings. [b]This ^{13}C resonance gives a triplet, hence only one RDC value was extractable. [c]For A_2 systems, $^1T_{HH} = 1.5 \cdot D_{HH}$. [d]Average of the two values, corrected for geminal ^{1}H−^{1}H couplings ($^2J_{H-C-H} = -10.8$ Hz for $CH_2\alpha$o and $^2J_{H-C-H} = -12.4$ Hz for $CH_2\beta$o; see Table S31, Supporting Information).[26]

3.3.2. Residual Dipolar Couplings. The values of the $^1J_{CH}$ scalar couplings used in the calculation of RDCs from eq 7 were taken to be 158.4 Hz for the inner and outer CH_{ar} groups, 141.0 Hz for the inner and outer $CH_2\alpha$ groups, and 125.0 Hz for all the other methylene and methyl groups of both the inner and outer rings.[24] These $^1J_{CH}$ values, along with the calculated dynamic frequency shifts, were accordingly subtracted from the observed $^1T_{CH}$ couplings. The experimental RDCs obtained from the ^{13}C and ^{1}H NMR spectra are given in Table 2.

The experimental RDC's can now be used for a calculation of the magnetic anisotropy similar to the procedure shown for the pseudocontact shift. Equation 6 for an axially symmetric complex **1** gets reduced to a simpler form, shown in eq 10:

$$D_{AB} = -\frac{\gamma_A \gamma_B h}{16\pi^3 {r_{AB}}^3} \frac{{B_0}^2}{15kT} \chi_a (3\cos^2\theta - 1) \quad (10)$$

The r_{AB} internuclear distances for ^{13}C−^{1}H in the methylene (1.093 Å) and aromatic (1.081 Å) groups or the ^{1}H−^{1}H distances were taken from the applied model (for a methylene group with d(C−H) equal to 1.093 Å and a H−C−H angle of 109.5°, the d(H−H) is 1.78486 Å). Although RDCs are deemed as not reliable enough for calculating the magnetic anisotropy susceptibility,[12e] we have calculated this value from the ^{13}C−^{1}H RDC of the CH_{ar}i group at 295.0 K, with the CH bond length fixed to 1.081 Å and with the assumption that the angle of this bond relative to the magnetic field axis is 90°. From eq 10, the calculated χ_a value was 13.75×10^{-31} m^3, which is of the same order of magnitude as determined from pseudocontact shifts (10.15×10^{-31} m^3), but somewhat larger. We attribute this discrepancy to limitations of our structural model, which was a single conformer for the description of an

dx.doi.org/10.1021/ja4069485 | J. Am. Chem. Soc. 2013, 135, 14349−14358

ensemble of conformers in solution. Similar discrepancies in the determination of χ_a from pseudocontact shifts as well as RDCs have been reported.[39]

The huge $^1T_{HH}$ measured for the $CH_2\alpha i$ and $CH_2\alpha o$ groups could only be justified with these vectors having the corresponding θ angles being close to a value of 0° (Figure S25, Supporting Information). This is due to the $(3\cos^2\theta - 1)$ term in eq 10, because of which the largest values of RDCs correspond to a $^1H-^1H$ vector being parallel or nearly parallel to the magnetic field axis. This orientation of the $^1H-^1H$ vector matches well with the model used to fit the pseudocontact shifts in ^{13}C and ^1H NMR spectra. Furthermore, as can be seen from Figure S25, Supporting Information, the only alternative orientation of the $^1H-^1H$ vector that would produce a large RDC is for the $CH_2\alpha$ $^1H-^1H$ vector to be oriented perpendicularly to the magnetic field axis. This orientation would make the two ^1H nuclei of the $CH_2\alpha o$ group equidistant from the two metal centers, which would result in both these groups having the same pseudocontact shift. The observed strong chemical shift difference of these protons demonstrate that this is not the case, that is, that this vector can only be approximately parallel to the magnetic field axis.

3.3.3. Mobility of the Butoxy Chains. It is common to express the mobility in terms of the generalized order parameter S, which takes values from 1.00 to 0.00.[40] The order parameter S is commonly calculated from T_1 relaxation times at different magnetic fields. This approach cannot be applied to compound **1**, because the relaxation is dominated by the distance to the unpaired electrons, that is, the distance to the terbium centers. The order parameter S was in our case calculated as the ratio of the experimentally observed RDC and the calculated value of the RDC on the basis of the structure determined by the pcs analysis (eq 11).

$$S = \frac{\mathrm{RDC}^{\mathrm{experimental}}}{\mathrm{RDC}^{\mathrm{calculated}}} \tag{11}$$

Using the model already established to fit the ^{13}C NMR data, we were able to calculate the expected value of the residual dipolar couplings for the rigid molecule. Then, by comparison of the expected and experimentally obtained values of the RDCs, it is possible to estimate the intramolecular mobility of a corresponding methylene or methyl group. The $^{13}C-^1H$ and $^1H-^1H$ residual dipolar couplings calculated from the model are reported in Tables S32 and S33, respectively, Supporting Information. We used the measured RDC of the rigid $CH_{ar}i$ as starting point for an order parameter S of 1.00. The order parameters obtained with eq 11 from $^{13}C-^1H$ RDCs are given in Figure 8 and Table S34, Supporting Information.

Figure 8 shows that the order parameters of the alkyl chains of the inner ring are only slightly larger than the order parameters of the alkyl chain of the outer ring, indicating that the mobility of the inner butoxy chain is hardly hampered by steric constraints. Among the methylene groups, the mobility decreases in the following order: $CH_2\alpha < CH_2\beta < CH_2\gamma$. The same approach as mentioned for the $^{13}C-^1H$ RDCs was used for analyzing the $^1H-^1H$ couplings, and these results are presented in Figure 9 and Table S35, Supporting Information.

The results in Figure 9 indicate that among methylene groups at equivalent positions along the alkyl chains of the inner and outer phthalocyaninato ligands ($CH_2\alpha i$ vs $CH_2\alpha o$; $CH_2\beta i$ vs $CH_2\beta o$) the mobilities are very similar. The methylene groups $CH_2\beta i$ and $CH_2\beta o$ groups clearly show a much higher mobility than either of the two α-methylene groups. For all four groups in Figure 9, the order parameter slightly decreases with an increase in temperature, which shows that our approach is able to describe reasonably the internal mobility within aligned molecules.

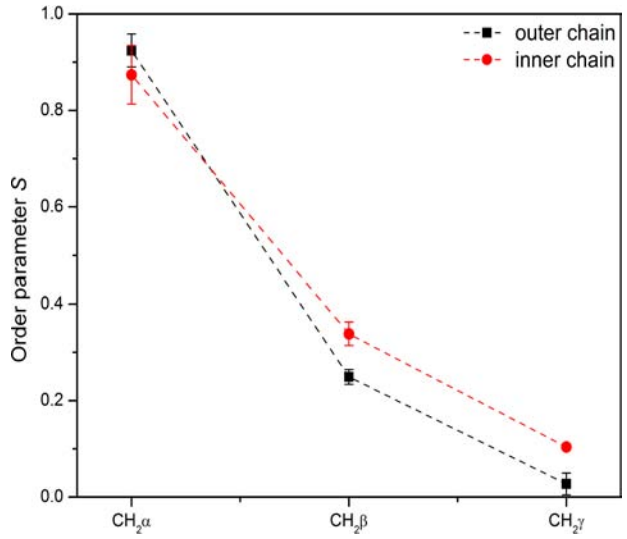

Figure 8. Calculated order parameters from $^{13}C-^1H$ residual dipolar couplings of the methylene groups of the inner and outer butoxy chains in **1**, obtained using the spectra recorded at 295.0 K. Order parameters of the groups of the inner ring are marked with circles, and data related to the groups of the outer phthalocyaninato ligand are marked with squares. Error bars reflect the uncertainties in measuring the exact values of $^1T_{CH}$ from the ^{13}C NMR spectra, due to either peak overlap or broad lines.

4. CONCLUSIONS

The terbium triple decker SMM $Tb_2(obPc)_3$ (**1**) was characterized in solution by ^{13}C and ^1H NMR spectroscopy. ^{13}C pseudocontact shifts, in combination with the X-ray structure of this complex, were used for the calculation of the axial component of the magnetic susceptibility tensor (χ_a = $(10.15 \pm 0.37) \times 10^{-31}$ m^3 at 295.0 K); χ_a was subsequently used to create a refined model of complex **1**, fitting the structure of this compound in solution. This model shows that pseudocontact contributions dominate the paramagnetic ^{13}C and ^1H NMR shifts of **1**, whereas Fermi-contact contributions are significant only for the carbon atoms of the phthalocyaninato ligands. The couplings observed in ^{13}C and ^1H NMR spectra were analyzed in terms of dynamic frequency shifts and residual dipolar couplings. The combination of the refined model with $^{13}C-^1H$ and $^1H-^1H$ residual dipolar couplings enabled insights into the mobilities of the individual groups of this complex.

Therefore a methodology for the combined analysis of pseudocontact shifts and residual dipolar couplings of lanthanide SMM's was developed. The information presented in this work should provide a foundation for further NMR investigations on lanthanide as well as d-block SMM's with single or multiple paramagnetic centers. The determination of magnetic anisotropy by two independent methods (pcs and RDC) makes the interpretation of paramagnetic NMR data in compounds where Fermi-contact interactions are considerably larger (e.g., d-block complexes) more reliable. Therefore, such nonstandard NMR analysis extends the toolbox for a

dx.doi.org/10.1021/ja4069485 | J. Am. Chem. Soc. 2013, 135, 14349−14358

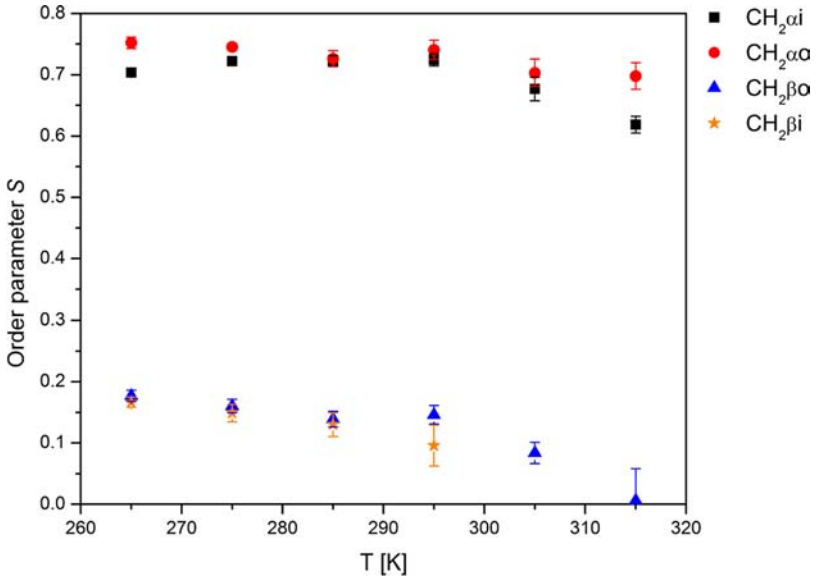

Figure 9. Calculated order parameters from ^{1}H−^{1}H residual dipolar couplings of the methylene groups of the inner and outer butoxy chains in **1**, obtained from the spectra recorded at 265.0−315.0 K. Error bars present the uncertainties in measuring the exact values of $^1T_{HH}$ from the ^{1}H NMR spectra, due to either peak overlap or broad lines. For the $CH_2\beta$i group, no couplings were observable at 305.0 K and at 315.0 K.

comprehensive understanding of paramagnetic molecules including single molecule magnets.

■ ASSOCIATED CONTENT

Supporting Information

^{1}H NMR and ^{13}C NMR spectra of complex **1**, tables containing chemical shifts, geometric coordinates, total couplings, RDCs, DFSs, order parameters, and details about the refined model of complex **1**, experimental data (e.g., NMR acquisition parameters), and additional information that is not listed in the main body of the paper. This material is available free of charge via the Internet at http://pubs.acs.org.

■ AUTHOR INFORMATION

Corresponding Author

markus.enders@uni-hd.de

Notes

The authors declare no competing financial interest.

■ ACKNOWLEDGMENTS

M.E. thanks the German-Japanese University Consortium (HeKKSaGOn) for travel support.

■ REFERENCES

(1) Caneschi, A.; Gatteschi, D.; Sessoli, R.; Barra, A.-L.; Brunel, L. C.; Guillot, M. *J. Am. Chem. Soc.* **1991**, *113*, 5873.

(2) (a) Sessoli, R.; Tsai, H. L.; Schake, A. R.; Wang, S.; Vincent, J. B.; Folting, K.; Gatteschi, D.; Christou, G.; Hendrickson, D. N. *J. Am. Chem. Soc.* **1993**, *115*, 1804. (b) Sessoli, R.; Gatteschi, D.; Caneschi, A.; Novak, M. A. *Nature* **1993**, *365*, 141. (c) Gatteschi, D.; Sessoli, R.; Villain, J. *Molecular Nanomagnets*; Oxford University Press: New York, 2006, and references therein. (d) Milios, C. J.; Vinslava, A.; Wernsdorfer, W.; Moggach, S.; Parsons, S.; Perlepes, S. P.; Christou, G.; Brechin, E. K. *J. Am. Chem. Soc.* **2007**, *129*, 2754. (e) Yoshihara, D.; Karasawa, S.; Koga, N. *J. Am. Chem. Soc.* **2008**, *130*, 10460. (f) Rinehart, J. D.; Long, J. R. *Chem. Sci.* **2011**, *2*, 2078. (h) Luzon, J.; Sessoli, R. *Dalton Trans.* **2012**, *41*, 13556.

(3) (a) Ishikawa, N.; Sugita, M.; Ishikawa, T.; Koshihara, S.-Y.; Kaizu, Y. *J. Am. Chem. Soc.* **2003**, *125*, 8694. (b) Ishikawa, N.; Sugita, M.; Ishikawa, T.; Koshihara, S.; Kaizu, Y. *J. Phys. Chem. B* **2004**, *108*, 11265. (c) AlDamen, M. A.; Clemente-Juan, J. M.; Coronado, E.; Marti-Gastaldo, C.; Gaita-Arino, A. *J. Am. Chem. Soc.* **2008**, *130*, 8874. (d) AlDamen, M. A.; Cardona-Serra, S.; Clemente-Juan, J. M.; Coronado, E.; Gaita-Arino, A.; Marti-Gastaldo, C.; Luis, F.; Montero, O. *Inorg. Chem.* **2009**, *48*, 3467.

(4) (a) Freedman, D. E.; Harman, W. H.; Harris, T. D.; Long, G. J.; Chang, C. J.; Long, J. R. *J. Am. Chem. Soc.* **2010**, *132*, 1224. (b) Zadrozny, J. M.; Xiao, D. J.; Atanasov, M.; Long, G. J.; Grandjean, F.; Neese, F.; Long, J. R. *Nat. Chem.* **2013**, *5*, 577.

(5) McInnes, E. J. L. *Struct. Bonding (Berlin)* **2006**, *122*, 69.

(6) (a) Arnold, D. P.; Jiang, J. *J. Phys. Chem. A* **2001**, *105*, 7525. (b) Ishikawa, N.; Iino, T.; Kaizu, Y. *J. Phys. Chem. A* **2002**, *106*, 9543. (c) Ishikawa, N.; Iino, T.; Kaizu, Y. *J. Am. Chem. Soc.* **2002**, *124*, 11440. (d) Ishikawa, N.; Sugita, M.; Tanaka, N.; Iino, T.; Kaizu, Y. *Inorg. Chem.* **2002**, *42*, 2440. (e) Ishikawa, N. *J. Phys. Chem. A* **2003**, *107*, 5831. (f) Ishikawa, N.; Iino, T.; Kaizu, Y. *J. Phys. Chem. A* **2003**, *107*, 7879. (g) Martynov, A. G.; Gorbunova, Y. G. *Polyhedron* **2010**, *29*, 391. (h) Birin, K. P.; Gorbunova, Y. G.; Tsivadze, A. Yu. *Magn. Reson. Chem.* **2010**, *48*, 505. (i) Martynov, A. G.; Gorbunova, Y. G.; Tsivadze, A. Yu. *Dalton Trans.* **2011**, *40*, 7165. (j) Birin, K. P.; Gorbunova, Y. G.; Tsivadze, A. Yu. *J. Porphyrins Phthalocyanines* **2011**, *15*, 667.

(7) (a) Evans, D. F. *J. Chem. Soc.* **1959**, 2003. (b) Grant, D. H. *J. Chem. Educ.* **1995**, *72*, 39.

(8) Relaxation of Zeeman terms, see Bertini, , I.; Luchinat, , C. In *Physical Methods for Chemists*, 2nd ed.; Drago, , R. S., Ed.; Saunders College Publishing: Fort Worth, TX, **1992**,; Chapter 12, p 500.

(9) Bertini, I.; Luchinat, C.; Parigi, G. *Prog. Nucl. Magn. Reson. Spectrosc.* **2002**, *40*, 249.

(10) Kruck, M.; Wadepohl, H.; Enders, M.; Gade, L. H. *Chem.—Eur. J.* **2013**, *19*, 1521.

(11) (a) Katoh, K.; Kajiwara, T.; Nakano, M.; Nakazawa, Y.; Wernsdorfer, W.; Ishikawa, N.; Breedlove, B. K.; Yamashita, M. *Chem.—Eur. J.* **2011**, *17*, 117. (b) Katoh, K.; Horii, Y.; Yasuda, N.; Wernsdorfer, W.; Toriumi, K.; Breedlove, B. K.; Yamashita. *Dalton Trans.* **2012**, *41*, 13582.

(12) (a) Bertini, I.; Luchinat, C. *Coord. Chem. Rev.* **1996**, *150*, 1. (b) Köhler, F. H. In *Magnetism: Molecules to Materials*; Miller, J. S., Drillon, M., Eds.; Wiley-VCH, Weinheim, Germany, 2001; pp 379−430. (c) Bertini, I.; Luchinat, C.; Parigi, G.; Pierattelli, R. *ChemBioChem* **2005**, *6*, 1536. (d) Rastrelli, F.; Bagno, A. *Chem.—Eur. J.* **2009**, *15*, 7990. (e) Kaupp, M.; Köhler, F. H. *Coord. Chem. Rev.* **2009**, *253*, 2376. (f) Bertini, I.; Luchinat, C.; Parigi, G. *Solution NMR*

of Paramagnetic Molecules - Applications to Metallobiomolecules and Models; Elsevier: Amsterdam, 2001.
(13) Jesson, J. P. The Paramagnetic Shift. In *NMR of Paramagnetic Molecules - Principles and Applications* La Mar, G. N., Horrocks, W., Holm, R. H., Jr., Eds.; Academic Press: New York, London, 1973.
(14) (a) Mao, J.; Zhang, Y.; Oldfield, E. *J. Am. Chem. Soc.* **2002**, *124*, 13911. (b) Fernandez, P.; Pritzkow, H.; Carbo, J. J.; Hofmann, P.; Enders, M. *Organometallics* **2007**, *26*, 4402. (c) Knorr, R.; Hauer, H.; Weiss, A.; Polzer, H.; Ruf, F.; Löw, P.; Dvortsák, P.; Böhrer, P. *Inorg. Chem.* **2007**, *46*, 8379. (d) Roquette, P.; Maronna, A.; Reinmuth, M.; Kaifer, E.; Enders, M.; Himmel, H.-J. *Inorg. Chem.* **2011**, *50*, 1942. (e) Kruck, M.; Sauer, D. C.; Enders, M.; Wadepohl, H.; Gade, L. H. *Dalton Trans.* **2011**, *40*, 10406. (f) Rastrelli, F.; Bagno, A. *Magn. Reson. Chem.* **2010**, *48*, 132.
(15) (a) Pennanen, T. O.; Vaara, J. *Phys. Rev. Lett.* **2008**, *100*, No. 133002. (b) Liimatainen, H.; Pennanen, T. O.; Vaara, J. *Can. J. Chem.* **2009**, *87*, 954. (c) Hrobárik, P.; Reviakine, R.; Arbuznikov, A. V.; Malkina, O. L.; Malkin, V. G.; Köhler, F. H.; Kaupp, M. *J. Chem. Phys.* **2007**, *126*, No. 024107.
(16) (a) Shirazi, A.; Goff, H. M. *Inorg. Chem.* **1982**, *21*, 3420. (b) Bertini, I.; Ciurli, S.; Dikiy, A.; Gasanov, R.; Luchinat, C.; Martini, G.; Safarov, N. *J. Am. Chem. Soc.* **1999**, *121*, 2037.
(17) (a) Reilley, C. N.; Wood, B. W.; Desreux, J. E. *Anal. Chem.* **1975**, *47*, 2110. (b) Reiley, C. N.; Good, B. W.; Allendörfer, R. D. *Anal. Chem.* **1976**, *48*, 1446. (c) Reuben, J. *J. Magn. Reson.* **1982**, *50*, 233. (d) Reuben, J.; Elgavish, G. A. *J. Magn. Reson.* **1980**, *39*, 421. (e) Shelling, J. G.; Bjorson, M. E.; Hodges, R. S.; Taneja, A. K.; Sykes, B. D. *J. Magn. Reson.* **1984**, *57*, 99. (f) Horrocks, W. D., Jr. *Inorg. Chem.* **1970**, *9*, 690. (g) Dobson, C. M.; Williams, R. J. P.; Xavier, A. V. *J. Chem. Soc., Dalton Trans.* **1973**, 2662.
(18) (a) Buchler, J. W.; Kihn-Botulinski, M.; Löffler, J.; Wicholas, M. *Inorg. Chem.* **1989**, *28*, 3770. (b) Ouali, N.; Rivera, J.-P.; Morgantini, P.-Y.; Weber, J.; Piguet, C. *Dalton Trans.* **2003**, 1251. (c) Rigault, S.; Piguet, C.; Bernardinelli, G.; Hopfgartner, G. *J. Chem. Soc., Dalton Trans.* **2000**, 4587. (d) Elhabiri, M.; Scopelliti, R.; Bünzli, J.-C. G.; Piguet, C. *J. Am. Chem. Soc.* **1999**, *121*, 10747. (e) Bleaney, B. *J. Magn. Reson.* **1972**, *8*, 91. (f) Kemple, M. D.; Ray, B. D.; Lipkowitz, K. B.; Prendergast, F. G.; Rao, B. D. N. *J. Am. Chem. Soc.* **1988**, *110*, 8275. (g) Morrill, T. C. In *Lanthanide Shift Reagents in Stereochemical Analysis*; Morrill, T. C., Ed.; VCH: New York, 1986. (h) Golding, R. M.; Halton, M. P. *Aust. J. Chem.* **1972**, *25*, 2577.
(19) (a) Weidong, H.; Wang, L. *Annu. Rep. NMR Spectrosc.* **2006**, *58*, 231. (b) Blackledge, M. *Prog. Nucl. Magn. Reson. Spectrosc.* **2005**, *46*, 23. (c) Lipsitz, R. S.; Tjandra, N. *Annu. Rev. Biophys. Biomol. Struct.* **2004**, *33*, 387. (d) Brunner, E. *Concepts Magn. Reson.* **2001**, *13*, 238. (e) Prestegard, J. H.; Al-Hashimi, H. M.l; Tolman, J. R. *Q. Rev. Biophys.* **2000**, *33*, 371. (f) Prestegard, J. H.; Bougault, C. M.; Kishore, A. I. *Chem. Rev.* **2004**, *104*, 3519. (g) Thiele, C. M. *Eur. J. Org. Chem.* **2008**, 5673. (h) Bax, A.; Kontaxis, G.; Tjandra, N. *Methods Enzymol.* **2001**, *339*, 127.
(20) (a) Lohman, J.; MacLean, C. *Chem. Phys.* **1978**, *35*, 269. (b) Lohman, J.; MacLean, C. *Chem. Phys.* **1979**, *43*, 144. (c) Oldfield, E.; Rothgeb, T. M. *J. Am. Chem. Soc.* **1980**, *102*, 3635. (d) Gayathri, C.; Bothner-By, A. A.; Van Zijl, P. C. M.; MacLean, C. *Chem. Phys. Lett.* **1982**, *87*, 192. (e) Bastiaan, E. W.; MacLean, C.; Van Zijl, P. C. M.; Bothner-By, A. A. *Annu. Rep. NMR. Spectrosc.* **1987**, *19*, 35. (f) Tolman, J. R.; Flanagan, J. M.; Kennedy, M. A.; Prestegard, J. H. *Proc. Natl. Acad. Sci. U.S.A.* **1995**, *92*, 9279. (g) Domaille, P. J. *J. Am. Chem. Soc.* **1980**, *102*, 5392. (h) Domaille, P. J.; Harlow, R. L.; Ittel, S. D.; Peet, W. G. *Inorg. Chem.* **1983**, *22*, 3944. (i) Van Zijl, P. C. M.; Ruessink, B. H.; Bulthuis, J.; MacLean, C. *Acc. Chem. Res.* **1984**, *17*, 172. (j) Strauss, S. H.; Long, K. M.; Magerstadt, M.; Gansow, O. A. *Inorg. Chem.* **1987**, *26*, 1185. (k) Facchine, K. L.; Staley, S. W.; Van Zijl, P. C. M.; Mishra, P. K.; Bothner-By, A. A. *J. Am. Chem. Soc.* **1988**, *110*, 4900.
(21) (a) Banci, L.; Bertini, I.; Huber, J. G.; Luchinat, C.; Rosato, A. *J. Am. Chem. Soc.* **1998**, *120*, 12903. (b) Déméné, H.; Tsan, P.; Gans, P.; Marion, D. *J. Phys. Chem. B* **2000**, *104*, 2259.
(22) Simon, B.; Sattler, M. *Angew. Chem.* **2002**, *114*, 453.
(23) In this paper, D_{AB} denotes the residual dipolar coupling between the two nuclei A and B, whereas D (without subscript) denotes the axial zero-field splitting parameter.
(24) Kalinowski, H.-O.; Berger, S.; Braun, S. *^{13}C-NMR-Spektroskopie*; Georg Thieme Verlag: Stuttgart, New York, 1984.
(25) There are two different definitions of D_{AB} in literature, which differ by a factor of 2. Consequently the factor of 16 in the denominator of equations 4 and 6 has to be replaced by 32 if D_{AB} is defined differently from eq. 7.
(26) (a) Pople, J. A.; Bothner-By, A. A. *J. Chem. Phys.* **1965**, *42*, 1339. (b) Bernstein, H. J.; Sheppard, N. *J. Chem. Phys.* **1962**, *37*, 3012. (c) Anet, F. A. L. *J. Am. Chem. Soc.* **1962**, *84*, 3767. (d) Barfield, M.; Grant, D. M. *J. Am. Chem. Soc.* **1961**, *83*, 4726. (e) Barfield, M.; Grant, D. M. *J. Chem. Phys.* **1962**, *36*, 2054. (f) Barfield, M.; Grant, D. M. *J. Am. Chem. Soc.* **1963**, *85*, 1899.
(27) Gossard, A. C.; Portis, A. M. *Phys. Rev. Lett.* **1959**, *3*, 164.
(28) Freeman, A. J.; Watson, R. E. *Phys. Rev. Lett.* **1961**, *6*, 343.
(29) Suhl, H. *Phys. Rev.* **1958**, *109*, 606.
(30) Nakamura, T. *Prog. Theor. Phys.* **1958**, *20*, 542.
(31) de Gennes, P. G.; Pincus, P. A.; Hartmann-Boutron, F.; Winter, J. M. *Phys. Rev.* **1963**, *129*, 1105.
(32) Buishvili, L. L.; Giorgadze, N. P.; Davituliani, A. A. *Sov. Phys.-JETP* **1975**, *41*, 1063.
(33) Goldman, M. *J. Magn. Reson.* **1984**, *60*, 437.
(34) (a) Tjandra, N.; Grzesiek, S.; Bax, A. *J. Am. Chem. Soc.* **1996**, *118*, 6264. (b) Bertini, I.; Luchinat, C.; Tarchi, D. *Chem. Phys. Lett.* **1993**, *203*, 445.
(35) Ghose, R.; Prestegard, J. H. *J. Magn. Reson.* **1997**, *128*, 138.
(36) Takahashi, K.; Shimoda, J.; Itoh, M.; Fuchita, Y.; Okawa, H. *Chem. Lett.* **1998**, *27*, 173.
(37) The oxygen atoms of the outer phthalocyanine ring have different positions in the X-ray structure, and we chose O atom nr. 2 for the attachment of the butyl chain. The oxygen atom nr. 2 represents an average position within the eight corresponding O atoms.
(38) Data from *Cambridge Structural Database*, see Allen, F. H.; Kennard, O.; Watson, D. G.; Brammer, L.; Orpen, A. G.; Taylor, R. *J. Chem. Soc., Perkin Trans. II* **1987**, 1.
(39) Tolman, J. R.; Flanagan, J. M.; Kennedy, M. A.; Prestegard, J. H. *Nat. Struct. Biol.* **1997**, *4*, 292.
(40) (a) Lipari, G.; Szabo, A. *J. Am. Chem. Soc.* **1982**, *104*, 4546. (b) Lipari, G.; Szabo, A. *J. Am. Chem. Soc.* **1982**, *104*, 4559.